Case Series

Augmented Reality to Guide Selective Clamping and Tumor Dissection During Robot-assisted Partial Nephrectomy: A Preliminary Experience

Riccardo Schiavina,[1,2] Lorenzo Bianchi,[1,2] Francesco Chessa,[1,2] Umberto Barbaresi,[1] Laura Cercenelli,[3,4] Simone Lodi,[5] Caterina Gaudiano,[6] Barbara Bortolani,[3] Andrea Angiolini,[1] Federico Mineo Bianchi,[1] Amelio Ercolino,[1] Carlo Casablanca,[1] Enrico Molinaroli,[1] Angelo Porreca,[7] Rita Golfieri,[6] Stefano Diciotti,[5] Emanuela Marcelli,[3] Eugenio Brunocilla[1,2]

Clinical Practice Points

- Three-dimensional (D) models can be used as additional preoperative tools to improve the understanding of the size, location, depth of a renal mass and vascular anatomy before robot-assisted partial nephrectomy (RAPN).
- During RAPN, the augmented reality (AR) technology with overlapping of 3D models inside the robotic console, can facilitate a fast and accurate anatomic identification of the renal vasculature and tumor anatomy in a real-time manner.
- The 3D-guided approach with AR during RAPN allows surgeon to perform selective and super-selective clamping in higher proportion of cases compared with conventional planning based on 2D imaging.
- The effective intraoperative management of renal hilum guided by AR guidance was performed as preoperatively planned in 86.7% of patients.
- Three-D models were more accurate than 2D standard imaging to evaluate the surgical complexity of renal masses according to nephrometry scores.
- The use of AR for 3D-guided renal surgery is useful to improve the intraoperative knowledge of renal anatomy with higher adoption of selective and super-selective clamping approach and safe surgical outcomes.

Clinical Genitourinary Cancer, Vol. ■, No. ■, ■-■

Keywords: Augmented reality, Renal cancer, Robotic partial nephrectomy, Selective clamping, 3D model

Introduction

Robot-assisted partial nephrectomy (RAPN) has been increasingly adopted in the treatment of T1 renal masses and lead to improve intraoperative and perioperative outcomes.[1-5] The preserved health renal parenchyma nearby the tumor is one of the most important predictors of long-term renal function,[6] whereas strong evidence concerning the ischemic damage to renal function are still lacking.[7] Nevertheless, to maximize the functional advantage of PN, different clamping approaches have been proposed.[8-10] Selective or super-selective clamping ideally induce ischemia targeted to the renal area near the tumor; however, this could result in longer operative time owing to the need of dissection of segmental arterial branches with

[1]Department of Urology, University of Bologna, Azienda Ospedaliero, Universitaria di Bologna, Bologna, Italia
[2]Department of Experimental, Diagnostic, and Specialty Medicine (DIMES), Cardio-Nephro-Thoracic Sciences Doctorate
[3]Department of Experimental, Diagnostic and Specialty Medicine (DIMES), Laboratory of Bioengineering
[4]Department of Biomedical and Neuromotor Sciences (DIBINEM), University of Bologna, Bologna, Italy
[5]Department of Electrical, Electronic, and Information Engineering, "Guglielmo Marconi," University of Bologna, Bologna, Italy
[6]Radiology Unit, Department of Diagnostic Medicine and Prevention, Azienda Ospedaliero-Universitaria di Bologna, Bologna, Italia
[7]Department of Urology, Abano Terme Hospital, Padua, Italy

Submitted: May 21, 2020; Revised: Aug 31, 2020; Accepted: Sep 7, 2020

Address for correspondence: Lorenzo Bianchi, MD, Department of Urology, University of Bologna, Azienda Ospedaliero-Universitaria di Bologna, Via Albertoni 15, Bologna, Italia
E-mail contact: lorenzo.bianchi3@gmail.com

https://doi.org/10.1016/j.clgc.2020.09.005

higher risk of vascular damage. Thus, conventional 2-dimensional (2D) cross-sectional images are unable to identify the exact intrarenal vascular anatomy and to predict the real tumor blood supply from segmental branches.[11] Recently, some authors reported that 3-dimensional (3D) models elaborated from conventional 2D imaging[11,12] can be used as additional tools to improve the understanding of the size, location, and depth of a renal mass and its vascular anatomy before PN.[13] The high-fidelity 3D reconstruction of renal vasculature allows the surgeon to be more confident with selective or super-selective clamping[14] and to change the preoperative plan based on 2D imaging toward a more selective clamping approach.[11,15] An additional step towards the precise medicine and imaging-guided surgery is the adoption of augmented reality (AR) in different surgical interventions.[16-22] During PN, the AR technology can facilitate a rapid and accurate anatomic identification of the renal vasculature.

In this case series, we evaluate the intraoperative application of AR to identify the main anatomic structures and to guide the surgical dissection and the level of the arterial clamping during RAPN.

Patients and Methods

Study Design, Participants, and Sample Size

We prospectively enrolled 15 consecutive patients with clinical diagnoses of T1 renal mass, scheduled for RAPN at our institution between December 2018 and June 2019. One single experienced robotic surgeon (R.S.) performed all the RAPN cases. Participants signed a written informed consent document. The study was approved by our Institutional Ethics Committee (IRB approval 3386/2018). The surgical complexity of the renal masses was scored according to PADUA[23] and R.E.N.A.L.[24] score based on conventional imaging. Then, PADUA and R.E.N.A.L. scores[25] for each lesion were re-assessed in a separate section, using the 3D virtual model. The preoperative surgical plan to define the level of arterial clamping (namely, no clamping, non-selective, selective [first branch], or super-selective [second or tertiary branch] clamping) was recorded by surgeon basing on the 2D conventional imaging and re-assessed after reviewing the 3D virtual model before surgery.

3D Modeling

To obviate bias owing to inaccurate 2D preoperative imaging, before surgery, all patients underwent high-quality chest and abdominal contrast-enhanced computed tomography (CT) at our institution (slice thickness, 1.25 × 2.5 mm; step interval, 0.8 × 2.0 mm) using angiography protocol. Intravenous non-ionic contrast material (Iomeprol 350 mg/mL, Iomeron; Bracco Imaging srl, Milan, Italy) was injected at a flow rate of 3 mL/s. The time delay to scanning was determined on the basis of the typical time to the renal arterial (25-30 seconds), parenchymal (80-100 seconds), and delayed (5-10 minutes) phases. All 3D virtual model reconstructions based on preoperative high-quality CT scans, were carried out by the Laboratory of Bioengineering of DIMES Department at the University of Bologna.

Multiple imaging series with different contrast levels were used for the selective identification of each anatomical structure of interest (healthy parenchyma, tumor lesion, arterial tree, renal veins, collecting system) in the image segmentation process. Segmentation (ie, the labeling of each structure of interest in each CT slice) was achieved using D2P software ('DICOM to PRINT'; 3D Systems Inc, Rock Hill, SC), a modular software package designed to convert DICOM patient medical images into 3D digital models, and CE-certified for the purpose of preoperative surgical planning.[15]

Manual refinement of the overall obtained automatic/semi-automatic segmentation output was carried out in 2 to 4 hours. The segmented anatomic structures arising from the multiple imaging series were then combined into 1 file using alignment of common regions, such as the healthy renal parenchyma that was segmented in all the series (Figure 1).

D2P was also used to obtain the 3D virtual models by converting the segmented structures to 3D triangulated surface mesh file, using mesh creation methods of D2P (contour or gridbase).

For each case, the surgeon viewed the 3D virtual model before the operation on a dedicated personal computer (PC) in the operating room.

AR Technique

An ad-hoc hardware and software setup (Figure 2) haves been implemented in order to develop an AR technique to guide robotic surgery. The surgical DaVinci video stream has been sent to a frame grabber (USB3HD, Startech, London, Ontario, Canada) connected to an AR-dedicated PC (equipped with an Intel i7 CPU, 8 GB RAM, and NVIDIA GeForce 840M video card), as previously described for prostatic surgery.[26] Thus, the received DaVinci video stream and a 3D view of the 3D virtual model (MeshMixer, Autodesk Inc, San Rafael, CA) have been overlapped in real-time (vMIX, StudioCoast Pty Ltd, Robina, Queensland, Australia). To this end, a biomedical engineer employed a 6 degrees of freedom (3D) mouse (SpaceMouse, 3D Connexion, Munich, Germany) for manipulating the 3D virtual model in order to achieve, in agreement with the surgeon, the best alignment with the Da Vinci video stream. The resulting AR video stream constituted of the 3D virtual model aligned and superimposed on the actual anatomic view provided by the Da Vinci video stream (AR-3D video stream) was then sent, in real-time, to a second monitor for quality control and, at the same time, imported inside the robotic console by TilePro.

Surgical Technique

RAPN was performed using the DaVinci Xi Surgical System (Intuitive Surgical Inc, Sunnyvale, CA) in a 4-arm configuration with the integrated Firefly fluorescence-imaging mode, as previously described.[3]

During intervention, the exact identification of the tumor's localization and the dissection of the renal hilum was guided by the AR-3D video stream, with the 3D virtual model manually oriented through the AR-dedicated PC by the assistant engineer. In case of a selective arterial clamping plan, 10 mg of indocyanine green was injected after 1 or more segmental vessels were clamped to assess if adequate ischemia of the tumor was achieved. If the ischemic area was not adequate, a non-selective clamp was then performed. After tumor resection, early unclamping was always performed between inner renorrhaphy and outer renorrhaphy, using the sliding clip technique as previously described.[27]

Statistical Analyses

The mean and standard deviation were reported for continuous variables. Frequencies and proportions were reported for categorical variables. Correlations between PADUA[23] and R.E.N.A.L.[24] scores

Figure 1 Example of the Process to Obtain the 3D Virtual Anatomical Model Using D2P Software (3D Systems) Starting From Patient CT Scan (A), by the Segmentation of the Renal Regions of Interest (B), to the Final 3D Renal Model (C)

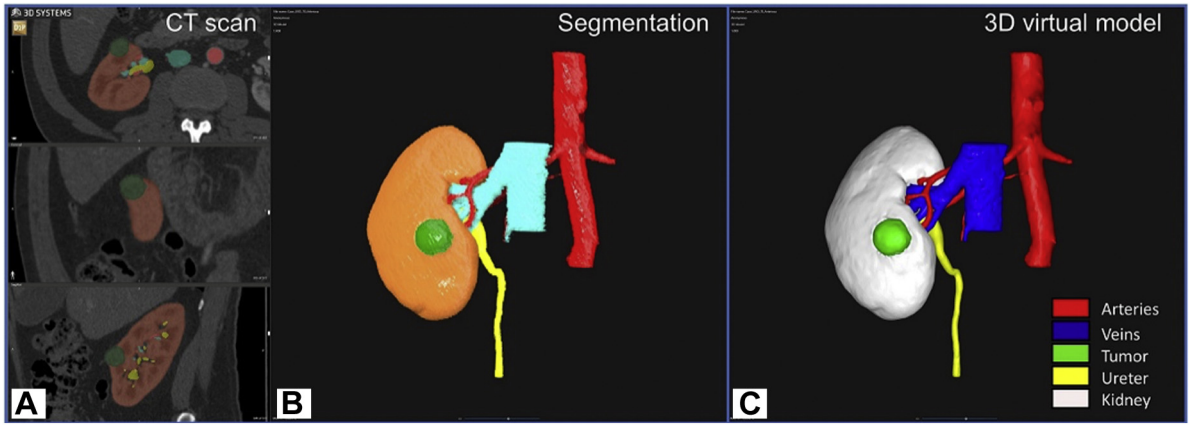

Abbreviations: CT = computed tomography; D2P = DICOM to PRINT (3D Systems Inc, Rock Hill, SC); 3D = 3-dimensional.

evaluated with and without the 3D model were calculated using the Pearson correlation coefficient. Preoperative plan of arterial clamping based on 2D conventional imaging, on the 3D model, and the effective intraoperative surgical approach to the renal hilum guided by the 3D-AR video were compared using the McNemar test. A *P*-value of $< .05$ was considered significant. All statistical tests were performed using SPSS 23.0 for Windows.

Results

Overall, 9 (60%) and 6 (40%) tumors were clinical T1a and T1b stage, respectively (see Supplemental Table 1 in the online version). After revision of the 3D virtual model reconstructions, PADUA and R.E.N.A.L. scores were reassessed in 9 (60%) and 8 (53%) cases, respectively (all $P \leq .04$) (see Supplemental Table 2 in the online version>). The plan of arterial clamping based on 2D preoperative imaging was recorded as follows: no clamping in 3 (20%), clamping of the main artery in 10 (66.7%), selective clamping in 1 (6.7%), and super-selective clamping in 1 (6.7%) cases. After revision of the 3D model, the plan of arterial clamping was modified as follows: no clamping in 1 (6.7%), clamping of the main artery in 2 (13.3%), selective clamping in 8 (53.3%), and super-selective clamping in 4 (26.7%) cases ($P = .03$) (Table 1). The intraoperative management of renal hilum was performed with the clampless, non-selective, selective, and super-selective approach in 2 (13.3%), 3 (20%), 7 (46.7%), and 3 (20%) patients, respectively. The effective intraoperative clamping approach guided by AR-guidance was performed as planned in 13 (86.7%) patients (Table 2). The median warm ischemia time (considering on clamp approach) was 9 minutes (IQR, 6-12 minutes). The mean $\pm$ SD estimated blood loss was 140 $\pm$ 190 mL. No positive surgical margins were observed, and 1 (6.7%) major (Clavien $\geq$ 3) postoperative complication was observed.

Discussion

Several points of our study are remarkable. First, in our study, we observed a significant difference between preoperative planning based on 2D conventional imaging and the reassessment of surgical planning after revision of the 3D model, resulting in a higher rate (80% vs. 13.4%) of selective and super-selective arterial clamping ($P = .03$). Accordingly, Bianchi et al[15] reported that the rate of intraoperative selective clamping was significantly higher in patients referred to PN with the use of 3D virtual models compared with individuals scheduled for preoperative planning based on conventional 2D imaging (57.1% vs. 13.3%; $P = .01$). Moreover, we found no significant differences between the preoperative plan of arterial clamping based on the 3D virtual model and the effective intraoperative approach to the renal hilum guided by AR ($P = .4$). Thus, the effective intraoperative management of renal hilum guided by AR was performed as preoperatively planned in 86.7% of patients. In 1 case, the super-selective plan of clamping was changed to a clampless approach owing to exophytic pattern of the renal mass, and in 1 patient, the selective clamping planned based on 3D model was changed to non-selective clamping owing to high fibrotic tissue at renal hilum with increased risk of vascular damage. Our results are consistent with those reported by Porpiglia et al.[14] Second, AR technology allows a fast and real-time overlapping of the 3D models inside the robotic console; thus, it can guide surgeons during arterial clamping and dissection without the need to temporarily stop the intervention to review the 3D model on a separate device.

Third, after revision of the 3D virtual reconstruction, PADUA[23] and R.E.N.A.L.[24] scores were reassessed in 9 (60%) and 8 (53%) cases, respectively (all $P \leq .04$), owing to the better comprehension of the tumor anatomy, as previously reported.[28] Fourth, the 3D virtual renal models with AR implementation were found to be feasible to represent the intraoperative vascular anatomy (see Supplemental Video in the online version). Finally, our 3D-planned RAPN proved to be safe, with no case of positive surgical margins. Moreover, 2 (13.3%) minor (Clavien 1-2) and only 1 (6.7%) major (Clavien $\geq$ 3) postoperative complications were observed: urinary linkage managed by ureteral stenting. In this case, the 3D model

Figure 2 A Schematic Diagram of the Hardware and Software Required to Implement the Intra-operative Use of AR to Guide Robotic Surgery. The Hardware Components Belonging to the Da Vinci Robot and the AR-Dedicated Devices are Grouped in Dashed Line Frames, Respectively. Moreover, in the "AR-Dedicated Devices" Frame, the Hardware Part of the Set-Up has Been Separated From the Software Running on the "AR-Dedicated PC"

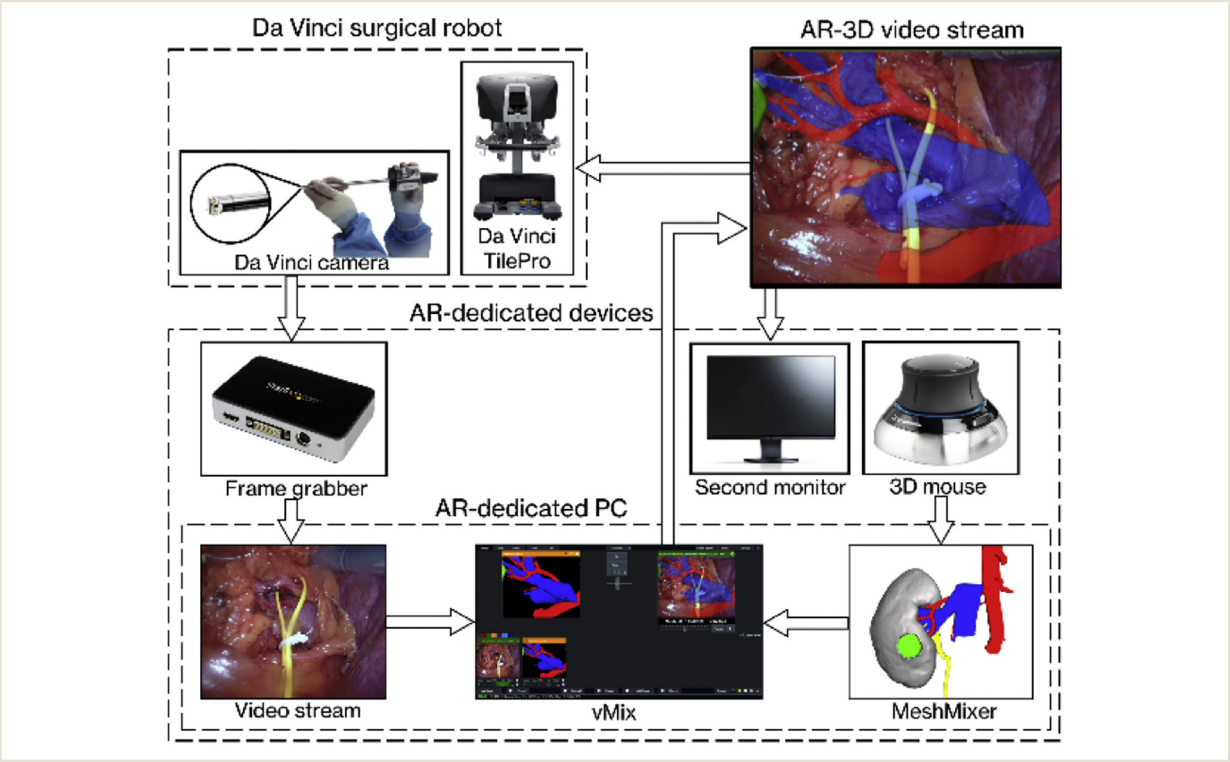

Abbreviations: AR = augmented reality; PC = personal computer; 3D = 3-dimensional.

revealed suspected collecting system involvement not detected by CT scan.

Our study is not void of limitations. First, the restricted number of patients included limits our results. Second, despite the 3D-AR model being feasible to reproduce renal anatomy, some variability between the model and the intraoperative findings could be related to the lack of precisely defining the consistency of tissues, to the patient's position on the surgical table, and to the surgical manipulation of tissues and organs. Third, the lack of a control group of patients who underwent RAPN without the use of AR did not allow to assess the real impact of this technology in modifying the surgical approach. Finally, the major limitations of AR-assisted surgery consist of possible registration inaccuracy, translating into a poor navigation precision and the need of manual external adjustments of

Table 1 Intended Level of Arterial Clamping Planned Based on Conventional 2D Imaging and on 3D Model and Evaluation of the Effective Intraoperative Approach With AR-assisted Surgery Compared With the Intended Clamping Approach Based on 3D Model (McNeamar Test)

	Pre-surgical Plan Based on 2D Imaging	Pre-surgical Plan Based on 3D Model	*P* Value	Pre-surgical Plan Based on 3D Model	Intraoperative Approach With Augmented Reality	*P* Value
Level of clamping, n (%)						
No clamping	3 (20)	1 (6.7)	.03	1 (6.7)	2 (13.3)	.4
Main artery	10 (66.7)	2 (13.3)		2 (13.3)	3 (20)	
Selective (first segmental branch)	1 (6.7)	8 (53.3)		8 (53.3)	7 (46.7)	
Super-selective (second-third segmental branch)	1 (6.7)	4 (26.7)		4 (26.7)	3 (20)	

Abbreviations: AR = augmented reality; D = dimensional.

Table 2 Intraoperative, Perioperative, and Pathologic Characteristics

	Overall, n (%)
WIT, min	
0	2 (13.3)
1-19	13 (86.7)
≥20	0 (0)
Median (IQR)	9 (6-12)
Intraoperative clamping approach as planned	
No	2 (13.3)
Yes	13 (86.7)
Intraoperative use of ICG	
No	5 (33.3)
Yes	10 (66.7)
Operative time, min	
Median (IQR)	135 (113-177)
Time of resection, min	
Mean ± SD	9 ± 7
Time of renal suturing, min	
Mean ± SD	12 ± 9
EBL, mL	
Mean ± SD	140 ± 190
Intraoperative complications	
No	13 (86.7)
Yes	2 (13.3)
Conversion to open RN	
No	15 (100)
Yes	0 (0)
Postoperative complications grade	
No complications	12 (80)
Clavien 1-2	2 (13.3)
Clavien ≥ 3	1 (6.7)
Positive surgical margins	
No	15 (100)
Yes	0 (0)
Length of stay, d	
Median (IQR)	5 (4-6)
Pathologic lesion diameter, cm	
Mean ± SD	3.6 ± 2.0
Pathology	
Benign	2 (13.3)
Clear cell carcinoma	9 (60)
Papillary carcinoma	2 (13.3)
Chromophobe carcinoma	1 (6.7)
Other malignancies	1 (6.7)
Pathologic stage	
pT1a	9 (60)
pT1b	5 (33.3)
pT3a	1 (6.7)
Follow-up time, mos	
Mean ± SD	4 ± 2
Postoperative serum creatinine at last follow-up, mg/dL	
Mean ± SD	0.85 ± 0.18

Abbreviations: EBL = estimated blood loss; ICG = indocyanine green; IQR = interquartile range; RN = radical nephrectomy; SD = standard deviation; WIT = warm ischemia time.

the 3D model on the surgical field.[15] The size and shape of the kidney during a PN also may vary both because of the surgeon's manipulation of the organ and the dissection of tissues.[29] Indeed, the 3D virtual model displayed in AR is manually moved and adjusted on the surgical field by an assistant near the surgical console with a dedicated computer and software for AR, with a potential impact on reducing the precision of the tracking and lengthening the surgical time. Thus, further efforts to improve the automatic registration of the virtual content (3D model) to the surgical view are expected by the future improvement of artificial intelligence technology.

Conclusion

The use of AR for 3D-guided renal surgery could be useful to improve the intraoperative knowledge of renal anatomy and the surgical outcomes of RAPN with higher adoption of selective and super-selective clamping approaches.

Disclosure

The project was supported by a Technology Research Grant by Intuitive Surgical, Inc for the development of augmented reality technology in robotic surgery. The authors have stated that they have no conflicts of interest.

Supplemental Data

Supplemental tables and video accompanying this article can be found in the online version at https://doi.org/10.1016/j.clgc.2020.09.005.

References

1. Ljungberg B, Albiges L, Abu-Ghanem Y, et al. European Association of Urology Guidelines on renal cell carcinoma: the 2019 update. *Eur Urol* 2019; 75:799-810.
2. Xia L, Wang X, Xu T, Guzzo TJ. Systematic review and meta-analysis of comparative studies reporting perioperative outcomes of robot-assisted partial nephrectomy versus open partial nephrectomy. *J Endourol* 2017; 31:893-909.
3. Bianchi L, Schiavina R, Borghesi M, et al. Which patients with clinical localized renal mass would achieve the trifecta after partial nephrectomy? The impact of surgical technique. *Minerva Urol Nefrol* 2020; 72:339-49.
4. Borghesi M, Dababneh H, et al. Small renal masses managed with active surveillance: predictors of tumor growth rate after long-term follow-up. *Clin Genitourin Cancer* 2015; 13:e87-92.
5. Borghesi M, Schiavina R, Gan M, et al. Expanding utilization of robotic partial nephrectomy for clinical T1b and complex T1a renal masses. *World J Urol* 2013; 31:499-504.
6. Maurice MJ, Ramirez D, Malkoç E, et al. Predictors of excisional volume loss in partial nephrectomy: is there still room for improvement? *Eur Urol* 2016; 70:413-5.
7. Volpe A, Blute ML, Ficarra V, et al. Renal ischemia and function after partial nephrectomy: a collaborative review of the literature. *Eur Urol* 2015; 68:61-74.
8. Gill IS, Eisenberg MS, Aron M, et al. "Zero ischemia" partial nephrectomy: novel laparoscopic and robotic technique. *Eur Urol* 2011; 59:128-34.
9. San Francisco IF, Sweeney MC, Wagner AA. Robot-assisted partial nephrectomy: early unclamping technique. *J Endourol* 2011; 25:305-8.
10. Klatte T, Ficarra V, Gratzke C, et al. A literature review of renal surgical anatomy and surgical strategies for partial nephrectomy. *Eur Urol* 2015; 68:980-92.

11. Schiavina R, Bianchi L, Borghesi M, et al. Three-dimensional digital reconstruction of renal model to guide preoperative planning of robot-assisted partial nephrectomy. *Int J Urol* 2019; 26:931-2.
12. Bianchi L, Schiavina R, Barbaresi U, et al. 3D Reconstruction and physical renal model to improve percutaneous punture during PNL. *Int Braz J Urol* 2019; 45:1281-2.
13. Wake N, Rude T, Kang SK, et al. 3D printed renal cancer models derived from MRI data: application in pre-surgical planning. *Abdom Radiol (NY)* 2017; 42:1501-9.
14. Porpiglia F, Fiori C, Checcucci E, Amparore D, Bertolo R. Hyperaccuracy three-dimensional reconstruction is able to maximize the efficacy of selective clamping during robot-assisted partial nephrectomy for complex renal masses. *Eur Urol* 2018; 74:651-60.
15. Bianchi L, Barbaresi U, Cercenelli L, et al. The impact of 3D digital reconstruction on the surgical planning of partial nephrectomy: a case-control study. still time for a novel surgical trend? *Clin Genitourin Cancer* 2020, S1558-7673(20)30078-1. [Online ahead of print].
16. Tang SL, Kwoh CK, Teo MY, Sing NW, Ling KV. Augmented reality systems for medical applications. *IEEE Eng Med Biol Mag* 1998; 17:49-58.
17. Bertolo R, Hung A, Porpiglia F, Bove P, Schleicher M, Dasgupta P. Systematic review of augmented reality in urological interventions: the evidences of an impact on surgical outcomes are yet to come. *World J Urol* 2020; 38:2167-76.
18. Meola A, Cutolo F, Carbone M, et al. Augmented reality in neurosurgery: a systematic review. *Neurosurg Rev* 2017; 40:537-48.
19. Battaglia S, Badiali G, Cercenelli L, et al. Combination of CAD/CAM and augmented reality in free fibula bone harvest. *Plast Reconstr Surg Glob Open* 2019; 7:e2510.
20. Badiali G, Cutolo F, Cercenelli L, et al. The VOSTARS Project: a new wearable hybrid video and optical see-through augmented reality surgical system for maxillofacial surgery. *Int J Maxillofac Surg* 2019; 48:1-14.
21. Bosc R, Fitoussi A, Hersant B, Dao TH, Meningaud JP. Intraoperative augmented reality with heads-up displays in maxillofacial surgery: a systematic review of the literature and a classification of relevant technologies. *Int J Oral Maxillofac Surg* 2019; 48:132-9.
22. Laverdière C, Corban J, Khoury J, et al. Augmented reality in orthopaedics: a systematic review and a window on future possibilities. *Bone Joint J* 2019; 101-B: 1479-88.
23. Ficarra V, Novara G, Secco S, et al. Preoperative aspects and dimensions used for an anatomical (PADUA) classification of renal tumours in patients who are candidates for nephron-sparing surgery. *Eur Urol* 2009; 56:786-93.
24. Kutikov A, Uzzo RG. The R.E.N.A.L. nephrometry score: a comprehensive standardized system for quantitating renal tumor size, location and depth. *J Urol* 2009; 182:844-53.
25. Schiavina R, Novara G, borghesi M, et al. PADUA and R.E.N.A.L. nephrometry scores correlate with perioperative outcomes of robot-assisted partial nephrectomy: analysis of the Vattikuti Global Quality Initiative in Robotic Urologic Surgery (GQI-RUS) database. *BJU Int* 2017. https://doi.org/10.1111/bju.13628, accessed October 7, 2020.
26. Schiavina R, Bianchi L, Lodi S, et al. Real-time augmented reality 3D-guided robotic radical prostatectomy: preliminary experience and evaluation of the impact on surgical planning. *Eur Urol Focus* 2020 Aug 31, S2405-4569(20)30217-0. [Online ahead of print].
27. Volpe A, Garrou D, Amparore D, et al. Perioperative and renal functional outcomes of elective robot-assisted partial nephrectomy (RAPN) for renal tumours with high surgical complexity. *BJU Int* 2014; 114:903-9.
28. Porpiglia F, Amparore D, Checcucci E, et al. Three-dimensional virtual imaging of renal tumours: a new tool to improve the accuracy of nephrometry scores. *BJU Int* 2019; 24:945-54.
29. Altamar HO, Ong RE, Glisson CL, et al. Kidney deformation and intraprocedural registration: a study of elements of image-guided kidney surgery. *J Endourol* 2011; 25:511-7.

Supplemental Data

Supplemental Table 1 Overall Patients' Characteristics

	N (%)
Total patients	15
Age, y	
Median (IQR)	63 (58-68)
Gender	
Male	6 (40)
Female	9 (60)
ASA score	
1	2 (13.3)
2	10 (66.7)
3	3 (20)
Lesion side	
Right	7 (46.7)
Left	8 (53.3)
Preoperative Hb, g/dL	
Mean ± SD	13.9 ± 1.6
Preoperative serum creatinine, mg/dL	
Mean ± SD	0.85 ± 0.18
Clinical stage	
cT1a	9 (60)
cT1b	6 (40)

Abbreviations: ASA = American Society of Anesthesiologists; Hb = hemoglobin; IQR = interquartile range; SD = standard deviation.

Supplemental Table 2 Classification of the Renal Masses' Surgical Complexity According to PADUA and R.E.N.A.L. Score Based on Conventional Imaging and the 3D Virtual Model

	Assessment on Conventional Imaging, n (%)	Assessment on 3D Virtual Model, n (%)	*P* Value
PADUA score			
6-7	4 (27)	5 (33)	.02
8-9	7 (47)	4 (27)	
10-14	4 (27)	6 (40)	
R.E.N.A.L. score			
4-6	6 (40)	6 (43)	.04
7-9	6 (40)	4 (27)	
10-12	3 (20)	5 (33)	

Abbreviation: 3D = 3-dimensional.